

Experiments in superconducting vortex avalanches

E. Altshuler^{a,b,*}, T.H. Johansen^{c,b}, Y. Paltiel^d, P. Jin^b, K.E. Bassler^e,
O. Ramos^a, G.F. Reiter^e, E. Zeldov^d, C.W. Chu^{b,f,g}

^a *Superconductivity Laboratory, IMRE, Physics Faculty, University of Havana, 10400 Havana, Cuba*

^b *Texas Center for Superconductivity, University of Houston, Houston, TX 77202-5002, USA*

^c *Department of Physics, University of Oslo, POB Blindern, N-0316 Oslo, Norway*

^d *Condensed Matter Physics Department, Weizmann Institute of Science, Rehovot 7610, Israel*

^e *Department of Physics, University of Houston, Houston, TX 77204-5005, USA*

^f *Lawrence Berkeley National Laboratory, Berkeley, CA 94720, USA*

^g *Hong Kong University of Science and Technology, Clear Water Bay, Kowloon, Hong Kong*

Abstract

We detect vortex avalanches in superconducting Nb when an external field is slowly ramped up. Through the combination of micro-Hall probe magnetometry and Magneto-optical imaging, we are able to visualize the magnetic field “landscape” where the “local” vortex avalanches take place. We measure the avalanche size statistics at several locations in the magnetic landscape, comprising a number of events orders of magnitude larger than previously reported. The distributions of avalanche sizes show a nearly power-law character, and their details are strikingly independent from the specific features of the “magnetic landscape” where they take place. Some experiments in order to find spatial-temporal correlations between avalanches are also presented.

© 2004 Elsevier B.V. All rights reserved.

Keywords: Critical state; Vortex dynamics; Avalanches; Self-organized criticality

1. Introduction

The study of “non-catastrophic” vortex avalanches has attracted more attention than ever in the last decade or so, perhaps fueled by the ideas of self organized criticality (SOC) [1]. Differently from avalanches in sandpiles—commonly used as SOC paradigm in the literature—vortex avalanches have negligible inertia, which offers a better match to the SOC theoretical scenario [2,3]. The experimental work started in 1995 with a paper by Field et al. [4] studying a low- T_c cylinder submitted to a slowly increasing external magnetic field. Vortex avalanches through the inner boundary of the

cylinder were indirectly measured using a pick up coil, and showed a power-law distribution of avalanche sizes, which the authors claimed as consistent with SOC ideas [1]. The magnetic flux involved in “internal” avalanches could be directly measured later with the use of microscopic Hall probes. Such experiments were performed by Zieve et al. [5], Nowak et al. [6], and Behnia et al. [7], and showed power or peaked distributions of avalanche sizes, depending on the measuring parameters. The relatively poor statistics on most of those measurements made it difficult to assess the nature of these distributions and, in turn, whether the systems matched the SOC scheme. A review of these experiments is given in [8].

In this paper, we report vortex avalanche measurements in superconducting Nb using a combination of magneto-optic (MO) imaging and micro-Hall probes. This choice of techniques allowed us to perform detailed measurements of vortex avalanches with unprecedented statistics at different, controlled locations of the

* Corresponding author. Address: Superconductivity Laboratory, IMRE, Physics Faculty, University of Havana, 10400 Havana, Cuba.

E-mail address: jea@infomed.sld.cu (E. Altshuler).

“magnetic landscape” in the sample. This allowed us also to examine the *robustness* of those distributions—another important ingredient of SOC ideas. In fact, we were able to find robust power laws with similar critical exponents at several, qualitatively different regions of the flux penetration landscape. We present here also some findings on the spatial-temporal correlations between avalanches along different directions in the samples.

2. Experimental

We studied Nb foils of dimensions $1.5 \times 1.5 \times 0.025$ mm³, at 4.8 K. The MO images at different magnetic fields applied perpendicularly to the foil were obtained using a Faraday-active ferrite garnet film mounted on top of the superconductor, which was viewed through cross polarizers in a microscope. While the external field was ramped from 0 to 3.5 kOe at 1 Oe/s using a superconducting magnet, the magnetic flux variations at different spots of the sample were detected by micro-Hall probe arrays located at different positions. Each array contained 11 probes of 10×10 μm² area each, allowing a resolution better than a single vortex (i.e., one flux quantum, 2.1×10^{-15} Tm²).

3. Results and discussion

Fig. 1 shows a typical MO image of one sample at 450 Oe. The magnetic field penetrates the sample as ridges or fingers advancing into the sample as the field is slowly increased. The cross-section of each of these fingers closely resembles an “inverted V” critical state profile, and their overall shape repeat as the experiment

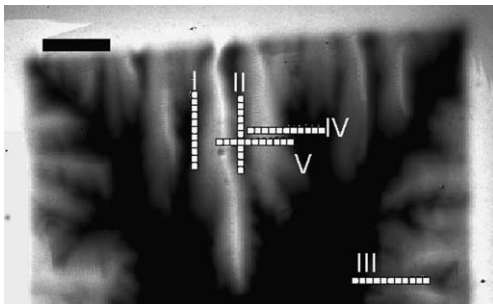


Fig. 1. Micro-Hall probe arrays on the flux penetration landscape. A MO image of approximately half sample area is shown at an applied field of 450 Oe at 4.8 K, on which the different locations of the micro-Hall probe arrays are indicated by white dots. As the magnetic field is increased, all the “ridges” observed in the magnetooptical picture grow gradually on a macroscopic scale. The scale bar is 0.2 mm long.

is repeated. Fig. 1 also shows as white dots the location of the Hall probe arrays we attached to the sample to measure the detailed avalanche dynamics at different locations within the “magnetic flux landscape”.

Fig. 2 shows typical data from one Hall sensor when a field is ramped up at 1 Oe/s. In spite of the fact that the overall structure looks smooth (and follows the prediction of the critical state model for perpendicular geometry [9]), the lower inset clearly shows that the flux enters the Hall area in distinct steps, which evidences the avalanche mechanism for vortex penetration. The height of a given step defines an avalanche of size s . The details of these steps do not repeat as the experiment is repeated, so quenched disorder is not the only parameter controlling the avalanche behaviour. The stochastic nature of the events was quantitatively demonstrated by calculating the correlations between the outputs of the same Hall probe from different runs under the same circumstances.

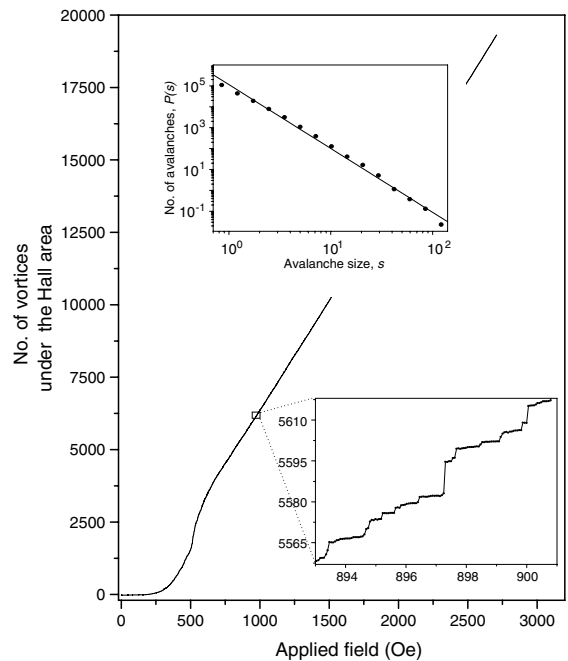


Fig. 2. Vortex avalanches measurements and statistics. The main curve is the output of the fourth Hall probe counting from the sample edge, in array I (see Fig. 4). It contains more than 4×10^4 datapoints. The lower inset shows a zoom from a tiny region of the main curve, clearly displaying distinct steps which reveals avalanche dynamics. The upper inset shows the avalanche size distribution constructed from the output of the 11 Hall probes in array I, comprising nearly 2×10^5 events. Steps smaller than one flux quantum were excluded from the event counting. The avalanche sizes were exponentially binned, so we get equally spaced points in the log–log plot. This distribution gives a critical exponent $\tau = 3.2 \pm 0.2$.

The upper inset in Fig. 2 shows a histogram from the signals recorded, in several runs, from the 11 probes in array I (see Fig. 1). The data include approximately 200 000 avalanche events—a number 100 times larger than in previous studies using Hall probes [5–7]. The number of avalanches, $P(s)$, versus their size, s , is seen to behave as a power law ($P(s) \sim s^{-\tau}$) for more than two orders of magnitude in s , and a critical exponent $\tau = 3.2 \pm 0.2$ was found.

The robustness of the avalanche dynamics was examined by determining the avalanche size distributions from the data provided by the rest of the Hall probe arrays (i.e., II, III, IV and V in Fig. 1). Array II is located parallel to the same central finger as array I, but has another finger by its side, so avalanches coming from the two neighbouring “hillsides” will contribute to the statistics. Probes in array III are also positioned parallel to two “competing” fingers. A top of the hill location is where the first four Hall probes in array IV, and probes 5, 6, 7 and 8 on array V (counting from the left) are mounted. In all cases, the avalanche statistics showed power laws for at least one and a half decades in the horizontal axis, and the critical exponent τ was quite similar for all cases. This robustness, together with the power laws found, strongly suggests that the vortex avalanche dynamics in our case can be described by the scenario of SOC.

A second set of experiments was performed to examine the correlation between avalanches along x , y and z . The measurements consisted in the simultaneous recording of the output at two different Hall probes while the field was ramped up.

Fig. 3 indicates several pairs of probes whose avalanche correlations were examined along the plane of the sample. Each pair was formed by a fixed probe (colored in black in the figure), and a second probe belonging to the same array (pointed by an arrow in the figure). The pairs under study in the case of array II (parallel to a long finger) were 4 & 5, 4 & 6, 4 & 7, 4 & 10 and 4 & 11. In the case of array IV (perpendicular to a long finger), they were 1 & 2, 1 & 3, 1 & 4, 1 & 6, 1 & 7 and 1 & 8. A graph similar to that shown in Fig. 2 was recorded simultaneously for probes n and m belonging to a given pair, and the following correlation function was then calculated in each case:

$$C(t') = k \frac{\langle \phi_n(t) \phi_m(t+t') \rangle - \langle \phi_n(t) \rangle \langle \phi_m(t) \rangle}{\sqrt{\sum [\phi_n(t) - \langle \phi_n(t) \rangle]^2 \sum [\phi_m(t) - \langle \phi_m(t) \rangle]^2}} \quad (1)$$

where t is the running time of the field sweep, ϕ_n and ϕ_m are the signal outputs of probes n and m , respectively, and k is a normalization factor. We find that the function $C(t')$ always display a peak near $t' = 0$, which means that the features of the two outputs were shifted in

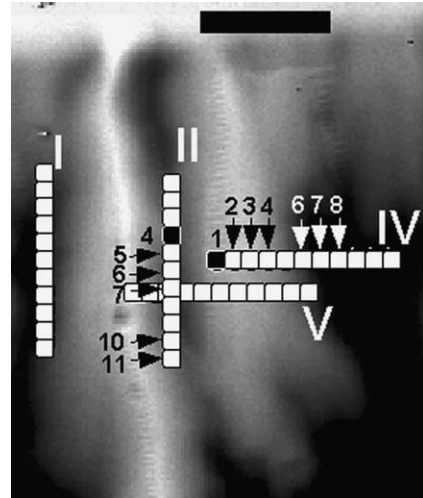


Fig. 3. Zoom of Fig. 1 indicating some of the pairs of probes between which avalanche correlations were measured. The probes indicated by black dots were the “fixed” members of the set of pairs under study within a given arrangement (see text). The scale bar is 0.15 mm long. Probes not indicated by arrows were not working properly at the time of the correlation experiments, so they were not used.

time—or applied field—by very small amounts. We will use the *height of that peak* as the single parameter that measures the correlation between probes n and m . Fig. 4 shows the resulting parameter at 4.8 K for different inter-probe distances plotted in the horizontal axis. The parameter representing the correlation decreases as the inter-probe distance increases with the same average slope along the fingers, and across them. The maximum of the correlation at 40 μm in the case of the transversal

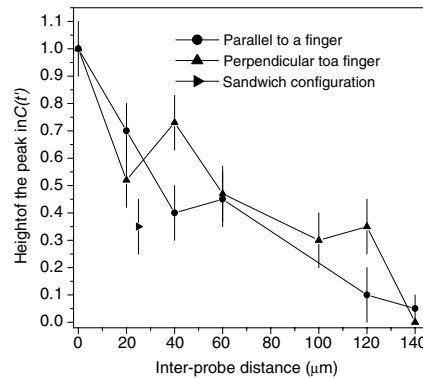


Fig. 4. Correlation results at 4.8 K for pairs of probes with different spatial configurations (see text and Fig. 3). Note that the centers between two consecutive probes within an array are 20 μm apart, and that the sample is 25 μm thick. The experimental misalignment along x and y of the two probes in the sandwich configuration, is estimated to be less than 30 μm .

direction could be related to the presence of the maximum of the longest finger at that point (see Fig. 3).

A third configuration not shown in Fig. 3 was examined in order to check the correlations along the direction of the applied field: it consisted in a “sandwich” where two probes were attached to opposite sides of the sample (so they were separated by a distance of 25 μm along z). It allowed us to show that there exists some correlation between avalanches on both sides of the sample (see Fig. 4), demonstrating that the vortex or vortex bundles involved in avalanche events are reasonably “rigid” objects, as SOC theory implicitly takes for granted. This results complements previous measurement in YBCO and BSCOO films by Lee and coworkers using an analogous sandwich configuration with less spatial resolution [10]. They measured the random telegraph signals and $1/f$ noise in thermally activated vortices without any Lorentz-like force. They determined that 20% to 60% of the vortices moved coherently at both sides of the sample, with no discernible dependence of the degree of coherence on sample thickness (below 100 μm) and temperature (below $0.9 T_c$). They concluded that coherent or incoherent vortex motion depends basically on the distribution of the pinning energies along the vortex line in their samples.

For all configurations, we examine separately the correlation parameter for small sized and big sized avalanches, demonstrating that the latter ones were much more correlated, as one could expect. We also performed the experiments within a range of temperatures between 4.8 and 8 K. The height of the correlation

peaks were quite temperature independent, except close to 8 K, where they approached zero. These observations further suggest the connection between our sandwich experiment and the results reported in [10].

Acknowledgements

The authors thank support from the World Laboratory Center for Pan-American Collaboration in Science and Technology, the Research Council of Norway, the National Science Foundation, the Israel Science Foundation—Center of Excellence Program, the “Alma Mater” grants program (University of Havana), the Department of Energy (USA) and the ACLS/SSRC study group on Cuba.

References

- [1] P. Bak et al., *Phys. Rev. Lett.* 59 (1987) 381–384.
- [2] C. Tang, *Physica A* 154 (1993) 315–320.
- [3] K.E. Bassler, M. Paczuski, *Phys. Rev. Lett.* 81 (1998) 3771–3774.
- [4] S. Field et al., *Phys. Rev. Lett.* 74 (1995) 1206–1209.
- [5] R.J. Zieve et al., *Phys. Rev. B* 53 (1996) 11849–11854.
- [6] E.R. Nowak et al., *Phys. Rev. B* 55 (1997) 11702–11705.
- [7] K. Behnia et al., *Phys. Rev. B* 61 (2000) R3815–R3818.
- [8] E. Altshuler, T.H. Johansen, *Rev. Mod. Phys.* 76 (2004) in print.
- [9] E. Zeldov et al., *Phys. Rev. B* 49 (1994) 9802–9812.
- [10] T.S. Lee et al., *Phys. Rev. Lett.* 74 (1995) 2796–2799.